DEVELOPMENT OF METHODOLOGY TO DOWNSCALE GLOBAL CLIMATE FIELDS TO 12-KM RESOLUTION

O. Russell Bullock, Jr.*, Kiran Alapaty, Jerry Herwehe, Megan Mallard, Tanya Otte
U.S. Environmental Protection Agency, Research Triangle Park, NC, USA

1. INTRODUCTION

Previous efforts to estimate future climate on fine scales have employed dynamical down-scaling where coarsely-resolved global-scale climate simulations were used to provide temporal and spatial boundary information for fine-scale meteorological models (Giorgi et al, 1990). One such climate down-scaling effort has been underway at the US EPA using the Weather Research and Forecast (WRF) model and a nested 108-/36-km modeling grid (Otte et al, 2012; Bowden et al., 2012). These studies have demonstrated WRF's capabilities in this regard by using the NCEP-Department of Energy Atmospheric Model Intercomparison Project (AMIP-II) Reanalysis data (Kanamitsu et al., 2002) as a surrogate for global climate model information and comparing the WRF model outputs to finer-scale re-analysis products.

To take these previous efforts one step further, this work applies a similar technique using WRF to provide information at 12-km horizontal resolution. Dynamical down-scaling to 12-km resolution involves challenges that were not encountered in the previous 108-/36-km work. These challenges include more than just higher computational and data storage demands, but also issues related to the resolution of surface features and the availability of adequately-resolved observational data for evaluation.

For this study, the WRF model is applied in three modes. The first is the standard WRF application where the simulation is constrained only by the provision of meteorological data at the lateral boundaries and surface conditions (e.g., topography, land surface type, sea-surface temperatures). For the other two modes, internal forcing is also applied. This internal forcing, also called interior nudging, is applied in two different ways called "analysis nudging" and "spectral nudging". The basis for all interior nudging is again the (AMIP-II) Reanalysis data, hereafter referred to as the R-2 data.

**Corresponding author:* O. Russell Bullock, Jr., U.S. Environmental Protection Agency, Mail Drop E243-01,109 T.W. Alexander Drive, Research Triangle Park, NC 27711; e-mail: bullock.russell@epa.gov

While analysis nudging on a fine grid based on much coarser information is known to damp high-resolution features, analysis nudging was found to be generally superior to spectral nudging at the 36-km scale with appropriate nudging parameters (Otte et al., 2012). This study investigates further adjustments to those parameters for 12-km WRF applications. Spectral nudging, when applied to appropriate wave numbers across the 12-km WRF domain, should not damp high resolution features like analysis nudging can. This study also investigates adjustments to the spectral nudging parameters to achieve optimal performance.

At the outset of this study, computational and data storage requirements for multi-year 12-km down-scaling were a concern. Thus we applied our down-scaling to only the year of 2006 during which over 11 million hourly surface observations of temperature, humidity and wind were available for model evaluation. We also used a limited horizontal model domain covering the United States east of the Rocky Mountains. Computing times for these 12-km simulations were about five times as long per simulated year compared to the previous studies. Nonetheless, a wide variety of tests were conducted to determine the most appropriate WRF model configuration for future long-term applications.

2. MODEL DESCRIPTION

The WRF model version 3.3.1 (WRF v3.3.1) was initialized at 0000 UTC 2 December 2005 to provide a 30-day spin-up time before the calendar year 2006 test period. The model was run continuously through 0000 UTC 1 January 2007. WRF was run on the 12-km domain with the same 34-layer configuration and 50 hPa model top used in Otte et al. (2012). Initial and lateral boundary data were derived from their 36-km analysis-nudged ("AN") simulation using standard WRF software. Input data for the lower boundary and for interior nudging (when applied) were the 2.5° × 2.5° R-2 analyses.

In general, the physics options used in Otte et al. (2012) are also used here. These include the Rapid Radiative Transfer Model for Global climate models (RRTMG; Iacono et al., 2008) for longwave and shortwave radiation, the Yonsei University planetary boundary layer (PBL) scheme (Hong et al., 2006), and the Noah land-surface model (Chen and Dudhia, 2001). We also used the WRF single-moment 6-class microphysics scheme (Hong and Lim 2006) in most of the 12-km simulations, but instead applied the Morrison double-moment scheme (Morrison et al., 2009) in two separate sensitivity tests. Most of the 12-km simulations used the Grell-3 convective parameterization scheme (Grell and Dévényi, 2002), but we also applied the Kain-Fritsch scheme (Kain, 2004) to test sensitivity to sub-grid convective parameterization.

Regarding interior nudging, three options were used: no nudging, analysis nudging and spectral nudging. Simulation test cases for which no interior nudging was used are designated with “NN”, cases where analysis nudging was used are designated with “AN”, and cases where spectral nudging was used are designated with “SN”.

The R-2 target data for nudging was of considerably coarser resolution (~250 km) than the 12-km model grid. In general, weaker analysis nudging is recommended for finer-resolved model grids (Stauffer and Seaman, 1994). Therefore we tested the analysis-nudging technique at 12-km resolution with nudging strengths varied between one-fourth and equal to the base values used by Otte et al. (2012) in their 36-km modeling. Analysis nudging was applied to horizontal wind components, potential temperature, and water vapor mixing ratio, and only above the planetary boundary layer (PBL).

Spectral nudging is scale selective based on selected maximum wave numbers in a spectral decomposition of the difference (target minus model) field. Spectral nudging was applied to the horizontal wind components, potential temperature, and geopotential, and only above the PBL. Sensitivity to the spectral nudging coefficients was tested with simulations using one-half and twice the base values chosen for 12-km modeling. A maximum wave number of two was selected for both horizontal dimensions to account for the small size of the 12-km domain and the limited resolution power of the R-2 data.

3. RESOLUTION OF SURFACE FEATURES

With the very first simulation of WRF at 12-km resolution the water temperature of inland lakes was an issue requiring attention. The standard method for setting lake surface temperatures in WRF uses a nearest-neighbor approach and sea-surface temperature data from the lower boundary input data. Strong discontinuities in the temperature of inland lakes were produced by this standard method. The Great Lakes are not resolved in the R-2 data. Many inland lakes in the central United States were assigned unreasonably warm water temperatures from the Gulf of Mexico. Other lakes just a short distance north were assigned cold water temperatures from James Bay. Another discontinuity running north-to-south across extreme eastern Lake Erie was also generated by this nearest-neighbor approach.

An alternative method for setting inland lake water temperatures was also tested. WRF Preprocessing System (WPS) software includes utility programs to set lake temperatures based on time-averaged surface air temperature. Fields of average surface air temperature were created for each month, starting in the month before the WRF simulation (November 2005). These fields of previous monthly average temperature were used to set all inland lake surface temperatures. While this did provide lake temperatures generally more reasonable at the start of the test period, other problems appeared later in the simulation. The alternate method produced a complete freeze-up of all Great Lakes by March. The Great Lakes might be better resolved by higher-resolution global GCMs, but smaller inland lakes will continue to remain unresolved and adversely affect simulations of meso-scale meteorology. We are currently working to realistically simulate within WRF the exchanges of thermal energy between lakes and the atmosphere above.

4. EVALUATION

4.1 Comparison to MADIS Surface Data

Previous down-scaling to 36-km resolution by Otte et al. (2012) used North American Regional Reanalysis (NARR) data at 32-km resolution to evaluate results. More highly resolved “ground-truth” data were required for this effort. Hourly observations of temperature, humidity and wind from the NOAA Meteorological Assimilation Data Ingest System (MADIS) were used. These data represent over 11,000,000 hourly observations across the 12-km WRF modeling domain during 2006. Comparisons of simulated and observed data were made using the Atmospheric Model Evaluation Tool (AMET) described in Appel et al. (2011).

The first evaluations performed were intended to gauge the improvements offered by 12-km WRF modeling over the previous 36-km results. As mentioned previously, the 36-km WRF results obtained with analysis nudging (AN) were deemed generally superior and were used to define the lateral boundary values for the 12-km modeling.

Figure 1 shows seasonal evaluations of mean bias and correlation for the parent 36-km WRF simulation and our base-case 12-km nested simulations with no interior nudging (NN), with analysis nudging (AN), and with spectral nudging (SN). Statistics in this comparison were based on model-observation pairs confined to a lat/lon window approximating the 12-km domain. Physics options in these base-case 12-km simulations were the same used in the 36-km study. Three-month seasons are defined as January-March (season 1) to October-December (season 4).

In general, the 12-km simulation with no interior nudging (NN) is less correlated to the observations and has greater error than the parent 36-km AN simulation. However, analysis or spectral nudging at 12-km resolution does improve these statistics for 2-meter temperature and, to a limited degree, 10-meter wind speed. This improvement with interior nudging is consistent with the results of Bowden et al. (2012), who found that nudging on the nested interior domain was necessary. A positive bias in water vapor is apparent in all runs and this bias is stronger in all of the 12-km simulations. This suggests that some physics options used at 36-km resolution might not be optimal for 12-km modeling. This issue is addressed in sensitivity tests described below.

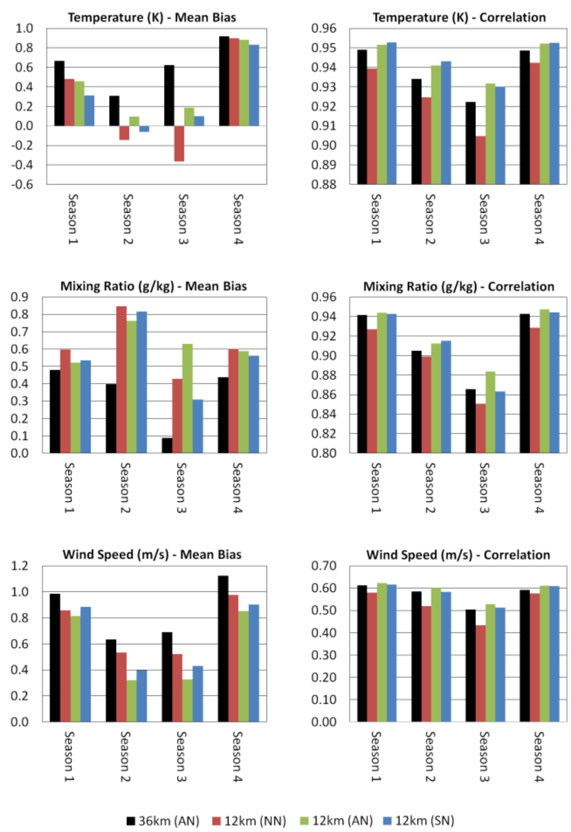

Fig. 1. Seasonal evaluations of mean bias and correlation for the 36-km parent simulation and the 12-km no-nudge (NN), analysis-nudge (AN) and spectral-nudge (SN) simulations.

4.2 Comparison to MPE Precipitation Data

Because of the high bias found for surface-level water vapor, it was critical to also investigate the simulated precipitation amounts. The Multisensor Precipitation Estimator (MPE) is a precipitation analysis system used by National Weather Service River Forecast Centers to produce gridded precipitation estimates for various hydrological applications. Observational data sources include weather radar data, automated rain gauges and satellite remote sensors. We obtained "Stage IV" data sets from the Earth Observing Laboratory at the National Center for Atmospheric Research. These provided hourly

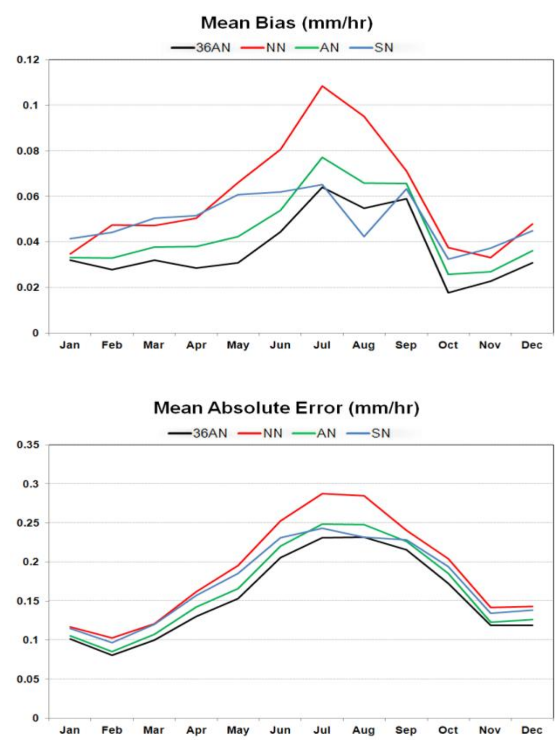

Fig. 2. Monthly mean bias and mean absolute error for WRF simulations as compared to the MPE precipitation data.

precipitation analyses at 4-km horizontal resolution that we re-analyzed to our 12-km and 36-km modeling domains using standard WRF Preprocessing System (WPS) software.

Figure 2 shows graphs of monthly mean bias and mean absolute error of WRF simulations compared to the MPE data. Hourly grids of MPE and WRF data were used to compile monthly statistics, thus the units for each of these graphs are mm hr^{-1}. It should be noted that the MPE data covered most, but not all, of the 12-km modeling domain. Also, the 36-km WRF simulation (from Otte et al. 2012) was truncated to the 12-km modeling domain to allow for proper comparison. All of the WRF simulations show a positive bias in precipitation for all months, with the greatest magnitudes in the summer months, especially July. The 12-km simulations show higher positive bias than the 36-km case in nearly all instances. The positive bias is most obvious for the no-nudge 12-km case. There was not as much difference in mean absolute error between the simulations. However, once again the 12-km cases showed greater deviation from the MPE data, especially when no nudging was applied.

Because the positive bias in simulated precipitation was most pronounced in the month of July, this month was chosen for further inspection. Figure 3 shows maps of mean bias in July 2006 for all four WRF simulations. The areal extent of the MPE data is evident in these plots. Also evident is an artificial gradient in MPE-indicated precipitation over the Atlantic continental shelf at the radial limit of weather radar coverage. This region over the Gulf Stream is known to experience strong convection and heavy

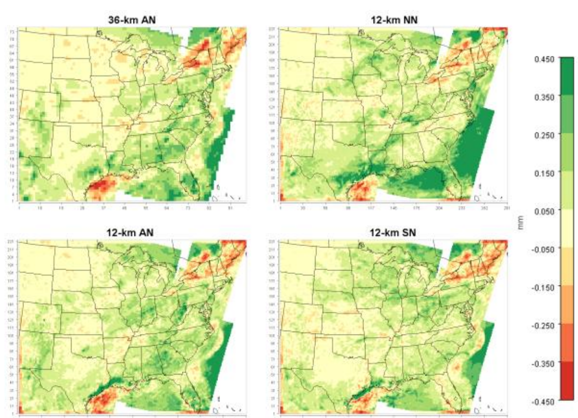

Fig. 3. Spatial maps of mean bias in simulated precipitation for July 2006 from the 36-km resolution WRF applying analysis nudging (36-km AN) and the 12-km WRF applying no nudging (12-km NN), analysis nudging (12-km AN) and spectral nudging (12-km SN).

precipitation that the MPE analysis does not appear to resolve well without radar guidance. The result is a very large spurious positive bias indicated for the WRF simulations in these locations that may be affecting the domain-wide statistics to some degree.

Over most land areas, precipitation bias is relatively moderate but still generally positive. The strong negative bias in the Northeast and New England regions is the result of spurious heavy precipitation indicated in the MPE data for only one or two hours during the month. It appears that more quality control is needed in the MPE data before any detailed analysis of model bias and error is possible for particular areas. Nonetheless, the work of Bowden et al. (2012) showed a strong tendency for the 36-km WRF to over-estimate precipitation in the Southeast region, especially in summer. This same over-estimation is evident in Figure 3 for the 36-km AN case. This positive bias is still quite evident in the 12-km NN case, but it appears to be moderated slightly by analysis nudging and reduced to a greater degree by spectral nudging.

4.3 Adjustments to Nudging Strength

As mentioned before, weaker nudging is recommended for WRF applications at finer scales. The values chosen for our base-case 12-km WRF simulations were reduced from those previously used for 36-km modeling, but that

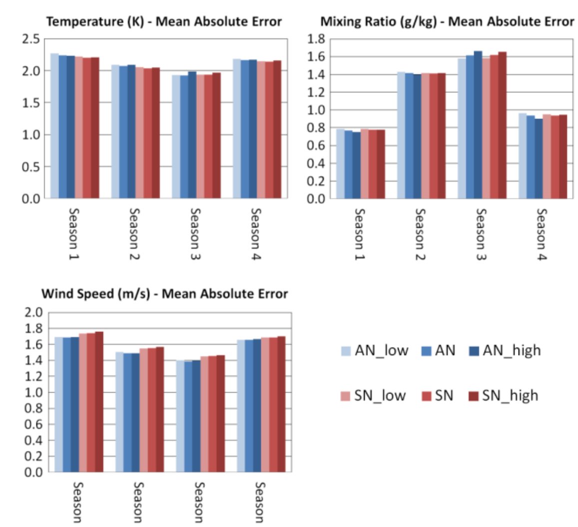

Fig. 4. Seasonal mean absolute error for WRF simulations testing nudging strength for analysis nudging (AN) and spectral nudging (SN). Low nudging strength is one-half the base value. High nudging strength is twice the base value.

reduction was somewhat arbitrary. To test model sensitivity to the choice of these analysis-nudging and spectral-nudging coefficients, values of one-half and twice the base values were also applied. Figure 4 shows seasonal mean absolute error for all six test cases (3 for analysis nudging, 3 for spectral nudging) for temperature, water vapor mixing ratio and wind speed.

Generally, the difference in model accuracy was very small for all three variables. Nonetheless, with only one exception, the base-value coefficients for both analysis and spectral nudging produced the lowest error in temperature for every season. But the same cannot be said for water vapor or wind speed. In season 3, water vapor error increased as nudging strength increased for both nudging methods. In season 4, water vapor error decreased with increasing analysis nudging strength. Note that nudging of water vapor is not performed with the spectral method. Nudging of water vapor has always been somewhat controversial and an in-depth investigation of the cause of these effects was not undertaken because of the relatively small differences in accuracy found. For wind speed, increasing the nudging strength nearly always resulted in an increase in mean absolute error. However, once again the changes in accuracy were relatively small.

Looking at mean bias, the results shown in Figure 5 suggest that model biases in water vapor and wind speed are increasingly corrected by both forms of nudging, analysis and spectral, as the nudging strength is increased. For temperature, this pattern of increasing correction of bias with increasing nudging strength only holds for season 4. For all other seasons, temperature bias is actually increased with stronger analysis nudging and mostly unaffected by changes in the strength of spectral nudging. The sensitivity of wind speed bias to nudging strength is rather low, but the general high bias in water vapor mixing ratio is more significantly corrected by stronger analysis or spectral nudging. Because water vapor is directly nudged in the analysis-nudging method, this result can be expected. However, the link between stronger spectral nudging (of temperature, wind and geopotential height) and reduced bias in water vapor is not direct and suggests complex interactions of model physics.

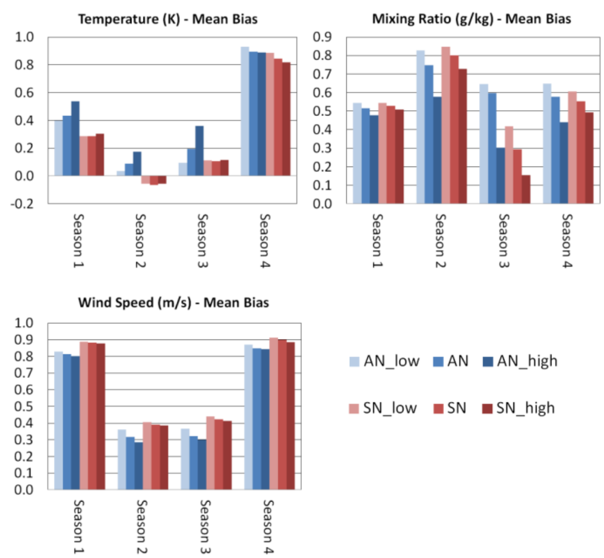

Fig. 5. Seasonal mean bias for WRF simulations testing nudging strength for analysis (AN) and spectral (SN) nudging. Low nudging strength is one-half the base value. High nudging strength is twice the base value.

4.4 Alternate Physics Options

Our base physics options included use of the Grell-3 sub-grid convection scheme. To test model sensitivity to this choice, we conducted test simulations using the Kain-Fritsch (K-F) scheme instead. No interior nudging was applied for either case so that the effect of the convective parameterizations could be better discerned. The results showed little difference in mean absolute error for temperature, water vapor mixing ratio or wind speed. The small differences that were noted suggest that the Grell-3 scheme was slightly superior.

Our base physics options also included use of the WRF Single-Moment 6-Class microphysics scheme (Hong and Lim 2006). To test model sensitivity, we instead applied the Morrison Double-Moment scheme (Morrison et al., 2009). Again, no interior nudging was applied for either of these simulations.

Figure 6 shows seasonal mean absolute error in temperature, water vapor mixing ratio and wind speed resulting from these two options. The

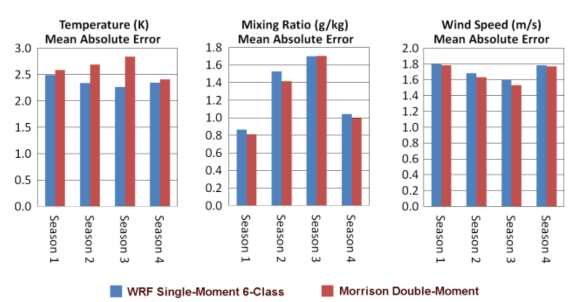

Fig. 6. Seasonal mean absolute error for simulations testing sensitivity to cloud microphysics scheme

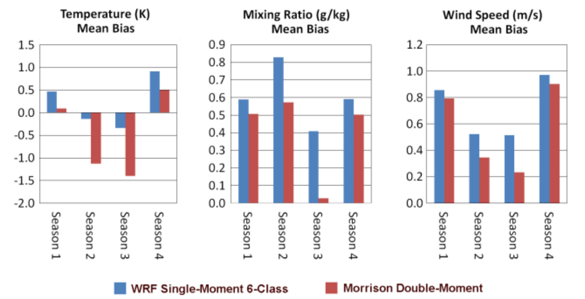

Fig. 7. Seasonal mean bias for simulations testing sensitivity to cloud microphysics scheme

Morrison scheme shows higher error in temperature, especially in season 3 (July-Sept). However, the error in water vapor is down slightly for all seasons except season 3.

Figure 7 shows seasonal bias results where the Morrison scheme is too cool in the warm seasons (seasons 2 and 3). The Morrison scheme also reduced the high bias in water vapor, especially in season 3. It appears that the lower surface temperatures resulting from the Morrison scheme may be causing less evaporation and thus lower water vapor mixing ratios. Correlation of simulated and observed temperature (not shown) was slightly lower in all seasons with the Morrison scheme, whereas correlation for water vapor and wind speed were little changed.

5. DISCUSSION AND SUMMARY

This work has attempted to apply a dynamical down-scaling technique previously developed for 36-km horizontal resolution to a finer 12-km resolution. While a variety of technical issues were encountered, the technique does appear to allow further refinement as long as proper adjustments are made to the interior nudging parameters. The exact adjustments that must be made depend on the seasons and meteorological variables of interest. It is clear that interior nudging is required in order to provide additional accuracy from down-scaling to 12-km resolution.

Optimum simulation of water vapor mixing ratio and precipitation at 12-km resolution may require a change in physics options from those applied previously at 36-km resolution. At 12-km resolution, we are near the point where larger convective elements may be resolved and the use of standard sub-grid convective parameterizations may be leading to positive precipitation bias through a sort of “double-counting” of precipitation mechanisms.

We intend to move forward with long-term applications of 12-km dynamical down-scaling with WRF once the issue of inland lake surface temperatures has been properly addressed. The computational and data storage resources required for 10- or 20-year simulations at 12-km resolution are daunting. However, more spatially refined climate projections have been identified as a critical need by hydrologic and urban air quality managers.

REFERENCES

Appel, K.W., R.C. Gilliam, N. Davis, A. Zubrow, and S.C. Howard, 2011: Overview of the atmospheric model evaluation tool (AMET) v1.1 for evaluating meteorological and air quality models. *Env. Modelling & Software*, **26**, 434-443.

Bowden, J.H., T.L. Otte, C.G. Nolte, and M.J. Otte, 2012: Examining Interior Grid Nudging Techniques Using Two-Way Nesting in the WRF Model for Regional Climate Modeling. *J. Climate*, **25**, 2805-2823.

Chen, F., and J. Dudhia, 2001: Coupling an advanced land surface–hydrology model with the Penn State NCAR MM5 modeling system. Part I: Model implementation and sensitivity. *Mon. Wea. Rev*., **129**, 569–585.

Giorgi, F., 1990: Simulation of regional climate using a limited area model nested in a general circulation model. *J. Climate*, **3**, 941–963.

Grell, G. A., and D. Dévényi, 2002: A generalized approach to parameterizing convection combining ensemble and data assimilation techniques. *Geophys. Res. Lett*., **29**, 1963

Hong, S.-Y., Y. Noh, and J. Dudhia, 2006: A new vertical diffusion package with an explicit treatment of entrainment processes. *Mon. Wea. Rev*., **134**, 2318–2341.

Hong, S.-Y., and J.-O. J. Lim, 2006: The WRF single-moment 6-class microphysics scheme (WSM6). *J. Korean Meteor. Soc*., **42**, 2, 129–151.

Iacono, M. J., J. S. Delamere, E. J. Mlawer, M. W. Shephard, S. A. Clough, and W. D. Collins, 2008: Radiative forcing by long-lived greenhouse gases: Calculations with the AER radiative transfer models. *J. Geophys. Res*., **113**, D13103, doi:10.1029/2008JD009944.

Kain, J.S., 2004: The Kain-Fritsch Convective Parameterization: An Update. *J. Appl. Meteor*., **43**, 170-181.

Kanamitsu, M., W. Ebisuzaki, J. Woollen, S.-K. Yang, J. J. Hnilo, M. Fiorino, and G. L. Potter, 2002: NCEP–DOE AMIP-II Reanalysis (R-2). *Bull. Amer. Meteor. Soc*., **83**, 1631–1643.

Morrison, H., G. Thompson, and V. Tatarskii, 2009: Impact of Cloud Microphysics on the Development of Trailing Stratiform Precipitation in a Simulated Squall Line: Comparison of One- and Two-Moment Schemes, *Mon. Weather Rev*., **137**, 991–1007.

Otte, T., C. Nolte, M. Otte, and J. Bowden, 2012: Does nudging squelch the extremes in regional climate modeling?. *J. Climate*. doi:10.1175/JCLI-D-12-00048.1, in press.

Stauffer, D. R., and N. L. Seaman, 1994: Multiscale four-dimensional data assimilation. *J. Appl. Meteor*., **33**, 416–434.